

Calcium-stimulated adenylyl cyclase subtype I is required for presynaptic long-term potentiation in the insular cortex of adult mice

Molecular Pain
Volume 15: 1–8
© The Author(s) 2019
Article reuse guidelines:
sagepub.com/journals-permissions
DOI: 10.1177/1744806919842961
journals.sagepub.com/home/mpx


Hui-Hui Miao^{1,2,3}, Xu-Hui Li^{2,3}, Qi-Yu Chen^{2,3}, and Min Zhuo^{2,3} 

Abstract

Recent studies indicate that presynaptic long-term potentiation in the anterior cingulate cortex may contribute to chronic pain-related anxiety. In addition to the anterior cingulate cortex, the insular cortex has also been indicated in chronic pain and its related emotional disorders. In the present study, we used a 64-channel multielectrode dish (MED64) system to record pre-long-term potentiation in the insular cortex. We showed that low-frequency stimulation paired with a GluKI-containing kainate receptor agonist induced N-methyl-D-aspartic acid receptor-independent pre-long-term potentiation in the insular cortex of wild-type mice. This form of pre-long-term potentiation was blocked in the insular cortex of adenylyl cyclase subtype I (ACI) knockout mice. Furthermore, a selective ACI inhibitor NB001 blocked pre-long-term potentiation in the insular cortex with a dose-dependent manner. Taken together, our results suggest that ACI contributes to pre-long-term potentiation in the insular cortex of adult mice and NB001 may produce anxiolytic effects by inhibiting pre-long-term potentiation in the anterior cingulate cortex and insular cortex.

Keywords

Presynaptic long term potentiation, insular cortex, adenylyl cyclase subtype I, mouse

Date Received: 26 February 2019; revised: 8 March 2019; accepted: 11 March 2019

Introduction

Patients with chronic pain often suffer from affective disorders such as anxiety, and anxiety may increase the likelihood of chronic pain development.¹ Among several cortical regions, the anterior cingulate cortex (ACC) and insular cortex (IC) are two key forebrain structures involved in pain perception and emotional response.^{2–4} Previous studies mainly focus on the ACC,^{5–7} and less studies have been carried out in the IC.

Long-term potentiation (LTP) serves as a key cellular model for chronic pain and anxiety.^{5–7} In both ACC and IC, different forms of LTP have been reported.^{6,8} Two major forms of LTP have been observed within the ACC: N-methyl-D-aspartic acid (NMDA) receptor-dependent postsynaptic LTP (post-LTP) and NMDA receptor-independent presynaptic LTP (pre-LTP).^{9–11} For pre-LTP in the ACC, the recent study suggested that it may play important roles in emotional anxiety

in chronic pain states.¹⁰ However, few studies investigated the pre-LTP in the IC.

Calcium-stimulated adenylyl cyclase subtype I (ACI) plays a critical role in the downstream of glutamate receptors and contributes to chronic pain-related neuronal plasticity in the ACC and IC.^{12,13} Application of a selective ACI inhibitor NB001 produced powerful analgesic effects in different chronic pain animal models due

¹Department of Anesthesia, Beijing Friendship Hospital, Capital Medical University, Beijing, People's Republic of China

²Center for Neuron and Disease, Frontier Institute of Science and Technology, Xi'an Jiaotong University, Xi'an, People's Republic of China

³Department of Physiology, Faculty of Medicine, University of Toronto, Toronto, Ontario, Canada

Corresponding Author:

Min Zhuo, Department of Physiology, Faculty of Medicine, University of Toronto, Medical Science Building, Room No. 3328, 1 King's College Circle, Toronto, Ontario M5S1A8, Canada.

Email: min.zhuo@utoronto.ca



to inhibition of pain-related post-LTP in the ACC and IC^{14–16}. Furthermore, our recent study showed that AC1 activity is required for the induction of pre-LTP in the ACC.¹⁰ However, it is not clear whether AC1 is required for pre-LTP in the IC. In the present study, we used an MED64 system, pharmacology, and gene knockout (KO) mice to investigate pre-LTP in the IC. We showed that AC1 contributed to the induction of pre-LTP in the IC by using *AC1* KO mice and an elective inhibitor for AC1, NB001. These observations are pertinent for the understanding of pain processing and anxiety-related mood disorders in the IC.

Materials and methods

Animals

Adult male C57BL/6 mice (7–10 weeks old) were purchased from Charles River. *AC1* KO mice with the C57BL/6 background were obtained from Dr Daniel R Storm (University of Washington, Seattle, WA). All animals were housed under a 12 h light/dark cycle with food and water provided ad libitum. All works were conducted according to the policy and regulation for the care and use of laboratory animals approved by Institutional Animal Care and Use Committee at University of Toronto.

Brain slice preparation

Adult male mice were anesthetized with isoflurane and the brains were removed and transferred to ice-cold artificial cerebrospinal fluid (ACSF) containing (in mM): 124 NaCl, 25 NaHCO₃, 2.5 KCl, 1 NaH₂PO₄, 2 CaCl₂, 1 MgSO₄ and 10 Glucose, pH 7.35–7.45. After 1 to 2 min cooling period, the brains were trimmed appropriately and glued onto the specimen disc of the vibrating tissue slicer (Leica VT1200S). Then, three IC slices (300 μ m) were gained and transferred to the recovery chamber with oxygenated (95% O₂, 5% CO₂) ACSF at room temperature for at least 1 h.

Preparation of the multielectrode array

The MED64 system (Panasonic Alpha-Med Sciences, Japan) was used in this study. The procedures for preparation of the MED64 system were the same as described before.^{17,18} Before using, the surface of the MED64 probe (MED-P515A, 8 \times 8 array, interpolar distance 150 μ m, Panasonic) was treated with 0.1% polyethyleneimine (Sigma-Aldrich) in 25 mM borate buffer, pH 8.4, overnight at room temperature.

Field potential recording

After 1 h of recovery, one IC slice was placed in a MED64 probe covering most of the 64 electrodes. When the slice was fixed, a fine mesh anchor (Warner Instruments, Harvard) was carefully placed to ensure slice stabilization during recording. The slice was continuously perfused with ACSF at a 2 to 3 ml/min flow rate. One planar microelectrode with monopolar constant-current pulses (0.2 ms in duration) was used for stimulation. The stimulation site was selected within the deep layer V region. Electrical stimulation was delivered to the stimulation channel and evoked field excitatory post-synaptic potentials (fEPSPs) were monitored and recorded from the other 63 channels. The intensity of the stimuli was adjusted so that 40% to 60% of the maximal amplitude of fEPSP was elicited in the channels closest to the stimulation site. The channels with the amplitude over -20 μ V were defined as activated channels and their responses were sampled every 2 min. Baseline responses were first recorded until the variation was $<5\%$ in most of the active channels within 1 h. Then, in the presence of the NMDA receptor antagonist (D(-)-2-amino-5-phosphonopentanoic acid (AP5), 50 μ M, 38 min), low-frequency stimulation (LFS, 2 Hz, 2 min) with a selective GluK1-containing kainate receptor agonist (amino-3-(3-hydroxy-5-tert-butylisoxazol-4-yl) propanoic acid (ATPA), 1 μ M, 18 min) was applied to the same stimulation site to induce pre-LTP. After LFS, the test stimulus was repeatedly delivered once every 2 min for 1 h to monitor the time course of pre-LTP.

Drugs

AP5 and ATPA were purchased from Hello Bio Inc. NB001 was provided by NeoBrain Pharmac Inc (Canada). AP5, ATPA, and NB001 were dissolved in distilled water. All of these drugs were diluted from the stock solutions to the final desired concentration in the ACSF before immediate use.

Data analysis

MED64 Mobius was used for data acquisition and analysis. For quantification of the LTP data, the initial slope of fEPSP was measured by taking the rising phase between 10% and 90% of the peak response, normalized and expressed as percentage change from the baseline level. The channels with at least the fEPSPs slopes increased 20% of baseline at the end of 20 min were defined as the LTP showing channels. For the paired pulse ratio (PPR), the ratio of the slope of the second response to the slope of the first response was calculated and averaged. For comparison between two groups, we used paired or unpaired Student's *t* test. For comparison

among three groups, we used one-way analysis of variance (ANOVA). All data are presented as means \pm SEM. In all cases, $p < 0.05$ was considered statistically significant.

Results

Pre-LTP of the IC

In our previous studies, we have shown that combined LFS (2 Hz, 2 min) with kainate receptor agonist (ATPA) produced NMDA receptor-independent pre-LTP in the ACC.^{19,20} Here, we wanted to see if similar pre-LTP could be found in the IC. The location of the 8×8 array MED64 probe electrodes within the IC slice is shown in Figure 1(a) and (b). The channel located on the deep layer V was chosen as the stimulation site (Figure 1(b), yellow dot). Activated channels with fEPSPs around the stimulation channel expressed from the superficial to deep layers of IC during baseline period (Figure 1(c)) and 1 h after pre-LTP induction (Figure 1(d)). After the baseline responses were stabilized for 20 min, we bath applied AP5 (50 μ M) for 20 min, before applying LFS (2 Hz, 2 min) in the presence of ATPA (1 μ M, 18 min) as described previously.¹⁹ The LFS was delivered 8 min after the onset of ATPA application. AP5 was always present during the pre-LTP induction process to exclude any contribution of postsynaptic NMDA receptor. We found that the combination of LFS with ATPA produced LTP lasting for at least 1 h (Figure 1(e) and (f)). As shown in an example, the fEPSP slope of one single channel (Channel 35) was potentiated to 165% of baseline at 1 h after LFS (Figure 1(e)). The averaged potentiation of nine pre-LTP showing channels from one IC slice reached $150 \pm 4\%$ of baseline at 1 h after pre-LTP induction (Figure 1(f)).

We then analyzed the expression of pre-LTP between superficial and deep layers in the IC. As shown in Figure 2(a), pre-LTP was obviously induced in superficial layers in the IC ($186 \pm 24\%$ of baseline, $n = 6$ slices/6 mice, $p < 0.01$, paired t test). Meanwhile, pre-LTP was also induced in deep layers in the IC (Figure 2(b), $189 \pm 12\%$ of baseline, $n = 6$ slices/6 mice, $p < 0.01$, paired t test). There was no significant difference in the amplitudes of potentiation of fEPSPs between the superficial and deep layers in the IC of wild-type (WT) mice (superficial vs. deep: $186 \pm 24\%$ vs. $189 \pm 12\%$, $n = 6$ slices/6 mice, unpaired t test, $p > 0.05$, Figure 2(c)).

Loss of pre-LTP in the IC of AC1 KO mice

Our previous studies have shown that AC1 is required for pre-LTP induction in the ACC.¹⁰ To determine whether AC1 is essential for pre-LTP induction in the IC, we performed the same pre-LTP induction protocol

in the IC slices of AC1 KO mice. As shown in Figure 3 (a), in the superficial layers of AC1 KO mice, combination of LFS with ATPA failed to induce any significant pre-LTP in the IC ($107 \pm 7\%$ of baseline, $n = 6$ slices/5 mice, $p > 0.5$, paired t test, black circles). Similarly, pre-LTP was abolished in the deep layers of AC1 KO mice ($107 \pm 8\%$ of baseline, $n = 6$ slices/5 mice, $p > 0.5$, paired t test, Figure 3(b), black circles). As compared with WT mice (Figure 3(a) and (b), black dots), pre-LTP in AC1 KO mice were absent in superficial layers (WT vs. AC1 KO: $186 \pm 24\%$ vs. $107 \pm 7\%$, six slices/six mice vs. six slices/five mice, $p < 0.01$, unpaired t test, Figure 3(c)) and deep layers (WT vs. AC1 KO: $189 \pm 12\%$ vs. $107 \pm 8\%$, six slices/six mice vs. six slices/five mice, $p < 0.01$, unpaired t test; Figure 3(c)). These results suggest that AC1 is required for the induction of pre-LTP in the IC.

Effects on PPR during pre-LTP in the IC

PPR is commonly used for measuring presynaptic function. As shown in Figure 4(a), sample traces revealing that ATPA combined with LFS significantly reduced the PPR 1 h after pre-LTP induction in IC slice of WT mice. Statistical results also showed that PPR (50 ms interval) was significantly decreased after pre-LTP induction in WT mice (baseline vs. 1 h after pre-LTP: 1.21 ± 0.04 vs. 1.11 ± 0.02 , $n = 6$ slices/6 mice, paired t test, $p < 0.05$, Figure 4(c)). Accordingly, sample traces of AC1 KO mice were demonstrated in Figure 4(b). However, the PPR in AC1 KO mice was not obviously changed after the pairing. Summarized data of PPR from AC1 KO mice were also not changed by the ATPA combined with LFS induction (baseline vs. 1 h after pre-LTP: 1.17 ± 0.06 vs. 1.20 ± 0.07 , $n = 6$ slices/5 mice, paired t test, $p > 0.05$, Figure 4(d)).

AC1 inhibitor NB001 blocked pre-LTP in the IC

Our previous study has shown that a selective AC1 inhibitor NB001 blocked pre-LTP in the ACC neurons.¹⁰ To test the requirement of AC1 activity for pre-LTP in the IC, we bath applied NB001 at the same time with AP5. NB001 we used has been purified to the level that is ready for human studies. As expected, we found that the pre-LTP expression was totally blocked in the presence of 5 μ M NB001 in the superficial layers of IC ($96 \pm 8\%$ of baseline, $n = 6$ slices/5 mice, $p > 0.5$, paired t test, Figure 5(a), black circles). Consistently, 5 μ M NB001 effectively blocked pre-LTP in deep layers of IC ($106 \pm 6\%$ of baseline, $n = 6$ slices/5 mice, $p > 0.5$, paired t test, Figure 5(b), black circles). Compared with WT mice (Figure 5(a) and (b), black dots), pre-LTP was attenuated with 5 μ M NB001 at 1 h after pre-LTP induction both in superficial layers (WT vs. 5 μ M NB001: $186 \pm 24\%$ vs. $96 \pm 8\%$, six slices/six

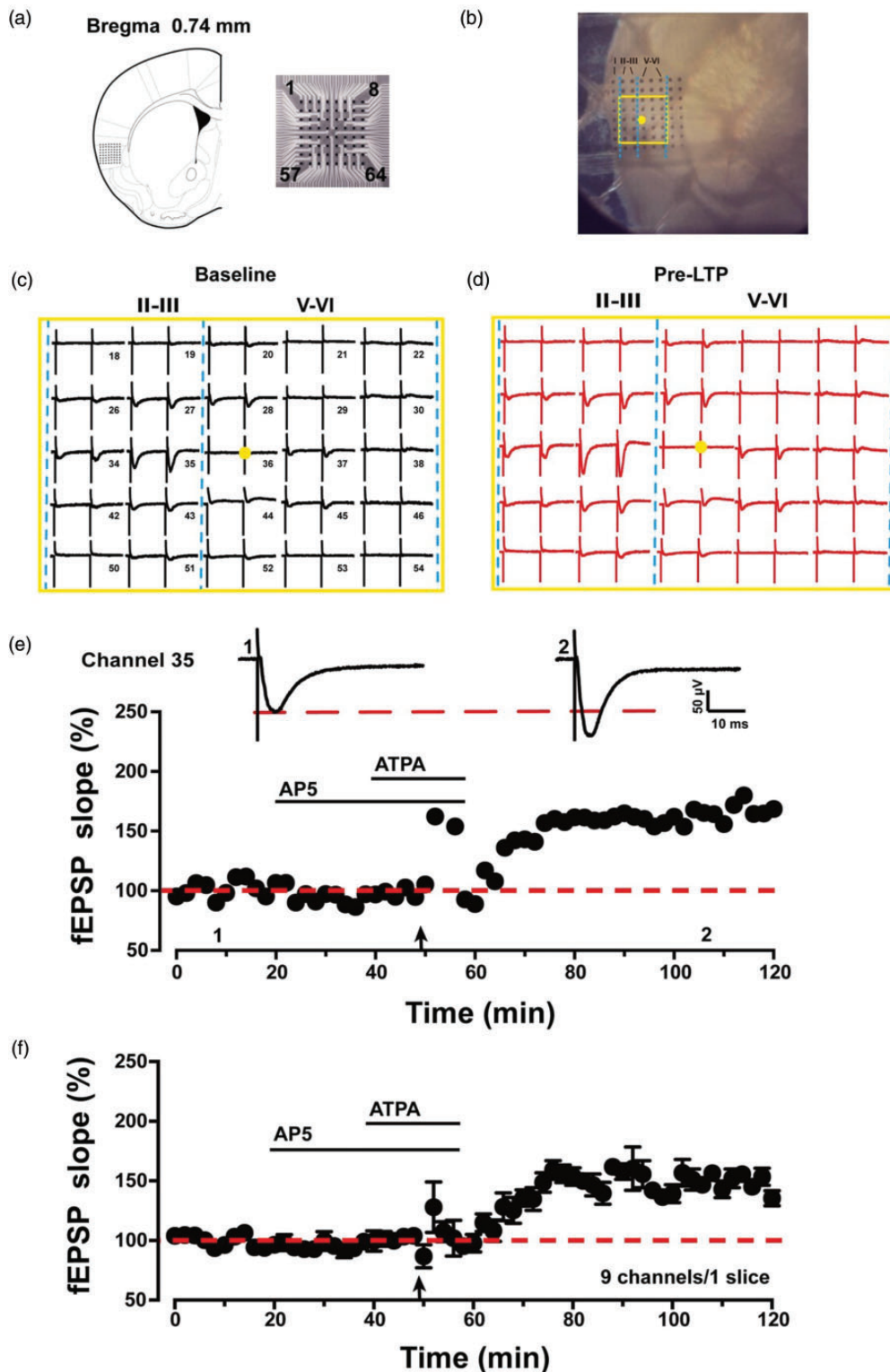


Figure 1. Spatial distribution and multisite synaptic responses of pre-LTP in the IC slice. (a) The location of MED64 probes on the IC slice (left, adapted from Paxinos and Franklin 2001, Bregma 0.74 mm) and the exhibition of the 8×8 electrodes (right). (b) Microscopic image of the MED64 probes on the IC slice. The yellow dot was the selected stimulation site and the yellow rectangle was the main activated region. (c) A general view of the spatial distribution of the potentials in all active channels within different layers (vertical lines) of one IC slice at baseline period. (d) An overview of the spatial distribution of the evoked potentials in all active channels across different layers (vertical lines) of one IC slice at 1 h after pre-LTP induction. (e) One sample trace and the time line of fEPSP slope for the pre-LTP are shown in one channel (channel 35). (f) The pooled time line of fEPSPs slopes of pre-LTP is shown in nine channels in one slice. Calibration: 50 μ V, 10 ms. LTP: long-term potentiation; ATPA: amino-3-(3-hydroxy-5-tert-butylisoxazol-4-yl) propanoic acid; AP5: D(-)-2-amino-5-phosphonopentanoic acid; fEPSP: field excitatory postsynaptic potential.

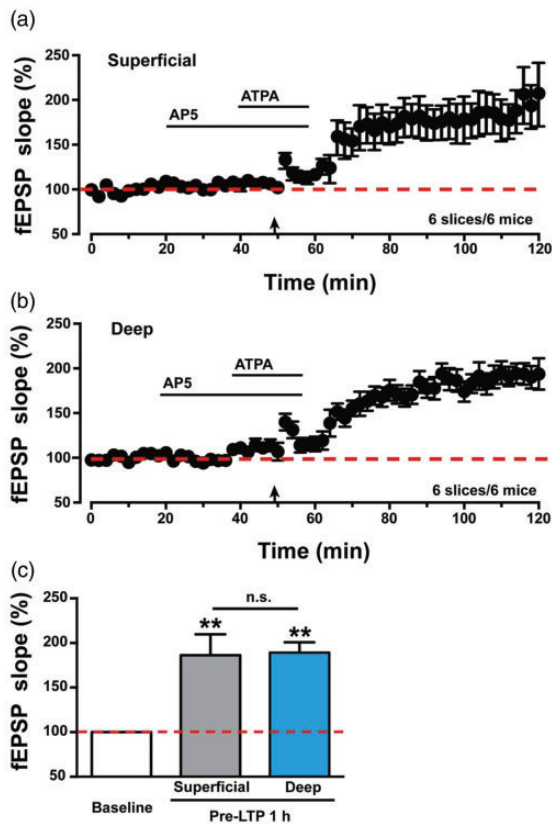


Figure 2. Summarized data of pre-LTP in the IC of WT mice. (a) Pooled data show fEPSPs slopes of pre-LTP in the superficial layers of IC in WT mice (six slices of six mice). (b) Pooled data show fEPSPs slopes of pre-LTP in the deep layers of IC in WT mice (six slices of six mice). (c) Statistical data of fEPSPs slopes to illustrate the potentials in superficial and deep layers at 1 h after pre-LTP induction comparing with baseline level. There was no significant difference of fEPSPs slopes between superficial and deep layers at 1 h after pre-LTP induction. The dashed line indicated the mean basal synaptic responses. $**p < 0.01$ means comparing with baseline. n.s. means no significant difference, error bars indicated SEM. LTP: long-term potentiation; ATPA: amino-3-(3-hydroxy-5-tert-butylisoxazol-4-yl) propanoic acid; AP5: D(-)-2-amino-5-phosphonopentanoic acid; fEPSP: field excitatory postsynaptic potential.

mice vs. six slices/five mice, $p < 0.01$, unpaired t test, Figure 5(a)) and deep layers (WT vs. 5 μ M NB001: $189 \pm 12\%$ vs. $106 \pm 6\%$, six slices/six mice vs. six slices/five mice, $p < 0.01$, unpaired t test, Figure 5(b)). We also calculated the change of PPR with 5 μ M NB001 during the pre-LTP induction. As shown in Figure 5(c), sample traces and statistical data show that the PPR was not significantly affected in the presence of 5 μ M NB001 by the ATPA combined with LFS induction in the IC (baseline vs. 1 h after pre-LTP: 1.20 ± 0.04 vs. 1.17 ± 0.06 , $n = 6$ slices/5 mice, paired t test, $p > 0.05$).

We also tested different doses of NB001 on the induction of pre-LTP in the IC. As shown in Figure 5(d), both

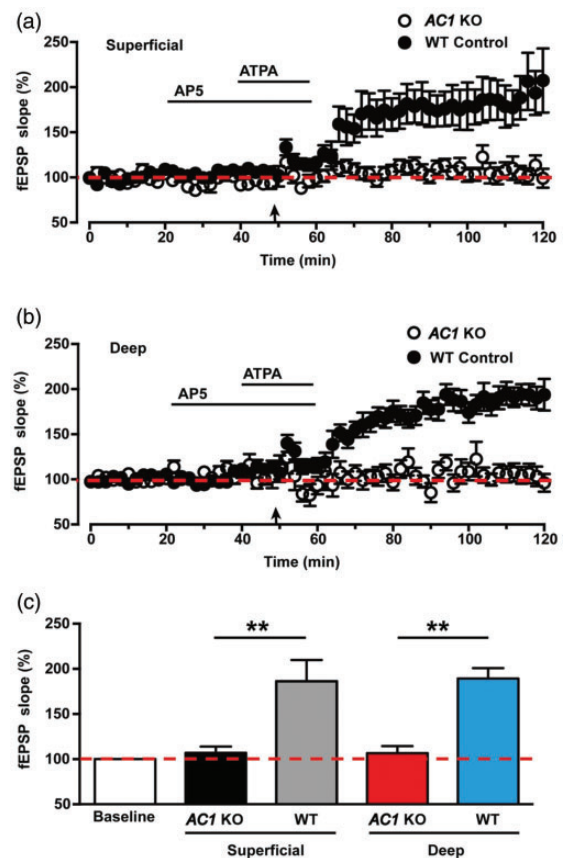


Figure 3. Pre-LTP was failed to induce in the IC of *AC1* KO mice. (a) Pooled data show that pre-LTP was attenuated in the superficial layers of the IC in *AC1* KO mice (open circles, six slices of six mice). The same data from WT mice in Figure 2(a) were plotted for comparison (filled circles). (b) Pooled data show that pre-LTP was abolished in the deep layers of the IC in *AC1* KO mice (open circles, six slices of six mice). The same data from WT mice in Figure 2(b) were plotted for comparison (filled circles). (c) Statistical results show the difference of averaged fEPSPs slopes between *AC1* KO mice and WT mice. The dashed line indicated the mean basal synaptic responses. $**p < 0.01$, error bars indicated SEM. ATPA: amino-3-(3-hydroxy-5-tert-butylisoxazol-4-yl) propanoic acid; AP5: D(-)-2-amino-5-phosphonopentanoic acid; fEPSP: field excitatory postsynaptic potential; KO: knockout; WT: wild-type; AC1: adenylyl cyclase subtype 1.

50 μ M NB001 ($95 \pm 4\%$ of baseline, $n = 6$ slices/5 mice, $p > 0.05$, paired t test) and 5 μ M NB001 ($105 \pm 5\%$ of baseline, $n = 6$ slices/6 mice, $p > 0.05$, paired t test) totally blocked the pre-LTP induction. Moreover, when we reduced the concentration to a low dose of 0.5 μ M, it still worked as partially blocking effect on the pre-LTP induction ($134 \pm 7\%$ of baseline, $n = 6$ slices/5 mice, $p > 0.05$, paired t test). There was significant difference of fEPSPs slopes among 50 μ M, 5 μ M and 0.5 μ M NB001 groups ($F_{(2,15)} = 13.99$, $p < 0.01$, one-way ANOVA with Tukey's post hoc). Taken together, these

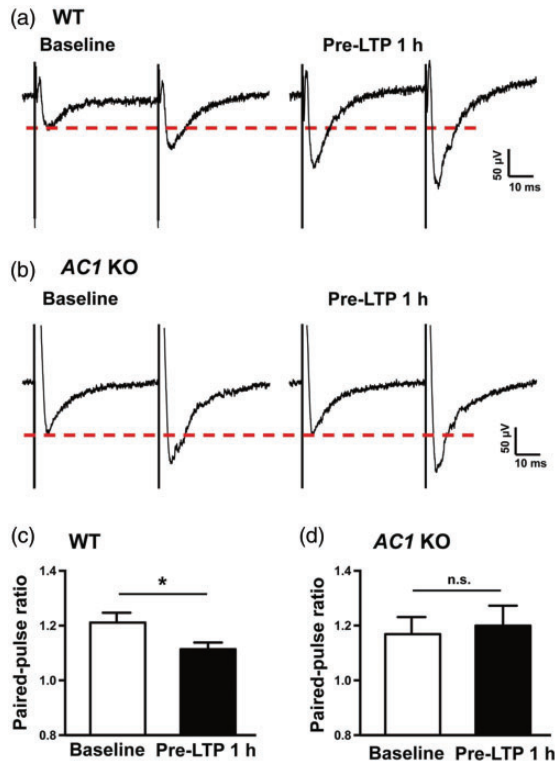


Figure 4. Different effects on paired pulse ratio during pre-LTP in the IC between *AC1* KO and WT mice. (a) Sample traces of the PPR before (left) and after pre-LTP induction (right) in the IC of WT mice. (b) Sample traces of the PPR before (left) and after pre-LTP induction (right) in the IC of *AC1* KO mice. (c) Statistical results show that PPR was significantly decreased at 1 h after pre-LTP induction compared with baseline in WT mice (six slices of six mice). (d) Statistical results show that PPR was not significantly changed at 1 h after pre-LTP induction compared with baseline in *AC1* KO mice (six slices of five mice). * $p < 0.05$, n.s. means no significant difference, error bars indicated SEM. Calibration: 50 μ V, 10 ms. KO: knockout; WT: wild-type; AC1: adenylyl cyclase subtype 1; LTP: long-term potentiation.

findings strongly suggest that AC1 is essential for the induction of pre-LTP in the IC.

Discussion

In this study, we identified the cortical pre-LTP in the adult mice IC by using the 64-channel multielectrode dish system. This form of LTP was presynaptically expressed and involved GluK1-containing kainate receptors but NMDA independently. Moreover, *AC1* KO mice failed to produce pre-LTP in the IC and a selective AC1 inhibitor NB001 blocked pre-LTP in the IC.

Recording of pre-LTP in the IC

Pre-LTP has been documented in the hippocampus and amygdala.^{21,22} The induction of pre-LTP in the ACC has been reported recently.¹⁰ By using the previously

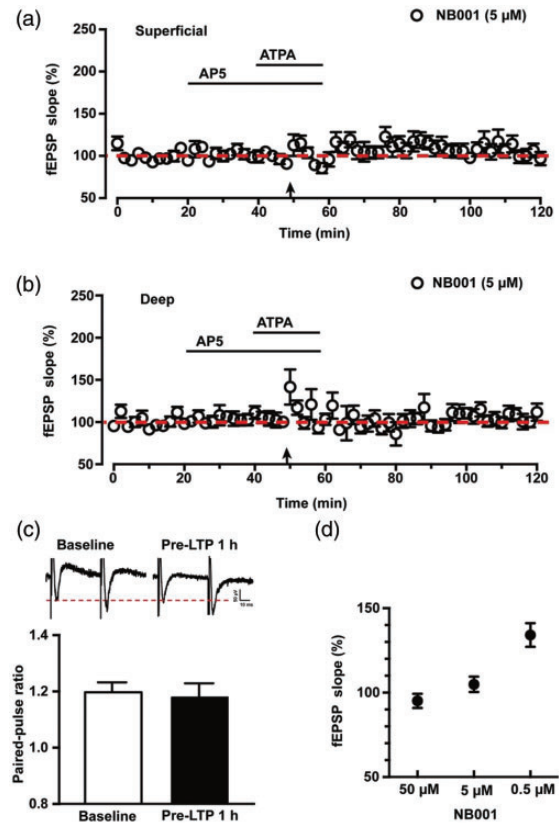


Figure 5. NB001 blocked the pre-LTP in the IC of WT mice. (a) Pooled data of fEPSPs slopes show that pre-LTP was totally blocked by 5 μ M NB001 in the superficial layers of IC (six slices of six mice). (b) Pooled data of fEPSPs slopes show that pre-LTP was effectively blocked by 5 μ M NB001 in the deep layers of IC (six slices of six mice). (c) Sample traces and statistical data show that PPR was not significantly changed during pre-LTP induction with 5 μ M NB001. (d) Summarized data show the blocking effect on the induction of pre-LTP with different doses of NB001 from 0.5 to 50 μ M. n.s. means no significant difference, Calibration: 50 μ V, 10 ms. LTP: long-term potentiation; ATPA: amino-3-(3-hydroxy-5-tert-butylisoxazol-4-yl) propanoic acid; AP5: D(-)-2-amino-5-phosphonopentanoic acid; fEPSP: field excitatory postsynaptic potential.

established MED64 recording system,⁸ we revealed that a combination of LFS (2 Hz, 2 min) with a kainate receptor agonist ATPA produced pre-LTP in the IC. This form of pre-LTP was NMDA receptor independent, which was consistent with previous observations in the ACC.^{19,20,23} Moreover, pre-LTP in IC was associated with changes in PPR, which was similar to recent studies in the ACC.^{10,22,23}

Requirement of AC1

This study provides strong genetic and pharmacological evidence that AC1 contributes to the IC pre-LTP. Pre-LTP was absent in the IC of *AC1* KO mice, furthermore,

pre-LTP was blocked by a selective AC1 inhibitor NB001 in the IC. This finding is similar to a recent study in the ACC.¹⁰ In addition to pre-LTP, post-LTP induced by theta burst stimulation (TBS) or pairing stimulation was totally abolished in cingulate pyramidal cells of *AC1* KO mice.²⁴ Pharmacological inhibition of AC1 with NB001 in ACC neurons also abolished post-LTP induced by pairing training.^{13,15} Additionally, Chen et al. found that AC1 was essential for the induction of late-phase LTP (L-LTP) in the ACC synapses.¹³ These results consistently demonstrate that calcium-stimulated AC1 play important roles in different forms of LTP in the ACC.⁵ Evidence for AC1 contribution in the IC has been found recently. We reported that AC1 is required for the induction of post-LTP in the IC.¹² Together with the current findings, it is likely that AC1 plays important roles in pain-related cortical plasticity such as pre- and post-LTPs in the IC and ACC of adult animals.

Role of IC in chronic pain and anxiety

Clinical studies had pointed out disease-related anxiety, especially in chronic pain conditions. In patients with post-traumatic stress disorder (PTSD), a chronic and debilitating anxiety disorder, enhanced chronic pain was often reported.²⁵ In patients with irritable bowel syndrome (IBS), IBS-related fear/anxiety significantly enhanced a patient's suffering from pain.²⁶ Consistent with this, it had been reported that techniques or manipulations that reduced anxiety and anxiolytic drugs were beneficial for reducing pain in chronic pain patients.²⁷ The IC received afferent projections from thalamic nuclei, and it formed reciprocal connections with the amygdala, limbic system, and cortical association areas.^{28–30} These anatomic connections provided the basis for its important roles in higher brain functions like pain perception, especially emotional and motivational components of pain. Moreover, it has been reported that the IC may be also related to PTSD, social anxiety disorders, fear, sadness, and phobias.^{2,31,32}

Pre-LTP in the ACC was considered taking part in pain-related anxiety, erasing pre-LTP by a pharmacological inhibitor of hyperpolarization-activated cyclic nucleotide-gated (HCN) channels produced inhibitory effects on injury-induced anxiety.¹⁰ Therefore, pre-LTP may constitute a synaptic mechanism by which anxiety and chronic pain interact. To induce pre-LTP in the IC, we used the same protocol as previously reported in the ACC. Anatomic evidence suggested that neurons in ACC and IC were likely interacted and both form bidirectional projections with neurons in the amygdala. We found that AC1 is similarly involved in LTP in both ACC and IC. Future studies are needed to investigate whether pre-LTP in the IC is also related to mood disorders and to investigate the possible interaction

between ACC and IC areas at molecular and behavioral levels.

In conclusion, these results demonstrate that kainate receptor-dependent form of pre-LTP is expressed in the IC and AC1 is required for IC pre-LTP. A selective AC1 inhibitor NB001 may produce anxiolytic effects by inhibiting pre-LTP in the IC and ACC.

Acknowledgment

The authors would like to thank Melissa Lepp for English editing.

Authors' contributions

HHM and XHL performed the experiments. HHM and MZ drafted the manuscript. MZ designed the project and finished the final version of the manuscript. All authors read and approved the final manuscript.

Declaration of Conflicting Interests

The author(s) declared no potential conflicts of interest with respect to the research, authorship, and/or publication of this article.

Funding

The author(s) disclosed receipt of the following financial support for the research, authorship, and/or publication of this article: This work was supported by grants from the Canadian Institute for Health Research (CIHR) Michael Smith Chair in Neurosciences and Mental Health, Canada Research Chair, CIHR operating grant (MOP-124807) and project grant (PJT-148648), Azrieli Neurodevelopmental Research Program and Brain Canada, awarded to MZ; by the National Science Foundation of China (81701040) and Beijing Talents Fund (2017000021469G258), awarded to HHM.

ORCID iD

Min Zhuo  <http://orcid.org/0000-0001-9062-3241>

References

1. Bushnell MC, Ceko M and Low LA. Cognitive and emotional control of pain and its disruption in chronic pain. *Nat Rev Neurosci* 2013; 14: 502–511.
2. Etkin A and Wager TD. Functional neuroimaging of anxiety: a meta-analysis of emotional processing in PTSD, social anxiety disorder, and specific phobia. *Am J Psychiatr* 2007; 164: 1476–1488.
3. Harris RE, Sundgren PC, Craig AD, Kirshenbaum E, Sen A, Napadow V and Clauw DJ. Elevated insular glutamate in fibromyalgia is associated with experimental pain. *Arthritis Rheum* 2009; 60: 3146–3152.
4. Zhuo M. Contribution of synaptic plasticity in the insular cortex to chronic pain. *Neuroscience* 2016; 338: 220–229.

5. Bliss TV, Collingridge GL, Kaang BK and Zhuo M. Synaptic plasticity in the anterior cingulate cortex in acute and chronic pain. *Nat Rev Neurosci* 2016; 17: 485–496.
6. Zhuo M. Cortical excitation and chronic pain. *Trends in Neurosciences* 2008; 31: 199–207.
7. Zhuo M. Neural mechanisms underlying anxiety-chronic pain interactions. *Trends in Neurosciences* 2016; 39: 136–145.
8. Liu MG, Kang SJ, Shi TY, Koga K, Zhang MM, Collingridge GL, Kaang BK and Zhuo M. Long-term potentiation of synaptic transmission in the adult mouse insular cortex: multielectrode array recordings. *J Neurophysiol* 2013; 110: 505–521.
9. Bliss TV and Collingridge GL. Expression of NMDA receptor-dependent LTP in the hippocampus: bridging the divide. *Mol Brain* 2013; 6: 5.
10. Koga K, Descalzi G, Chen T, Ko HG, Lu J, Li S, Son J, Kim T, Kwak C, Haganir RL, Zhao MG, Kaang BK, Collingridge GL and Zhuo M. Coexistence of two forms of LTP in ACC provides a synaptic mechanism for the interactions between anxiety and chronic pain. *Neuron* 2015; 85: 377–389.
11. Li XH, Miao HH and Zhuo M. NMDA receptor dependent long-term potentiation in chronic pain. *Neurochemical Research* 2019; 44: 531–538.
12. Yamanaka M, Matsuura T, Pan H and Zhuo M. Calcium-stimulated adenylyl cyclase subtype 1 (AC1) contributes to LTP in the insular cortex of adult mice. *Heliyon* 2017; 3: e00338.
13. Chen T, O'Den G, Song Q, Koga K, Zhang MM and Zhuo M. Adenylyl cyclase subtype 1 is essential for late-phase long term potentiation and spatial propagation of synaptic responses in the anterior cingulate cortex of adult mice. *Mol Pain* 2014; 10: 65.
14. Zhang MM, Liu SB, Chen T, Koga K, Zhang T, Li YQ and Zhuo M. Effects of NB001 and gabapentin on irritable bowel syndrome-induced behavioral anxiety and spontaneous pain. *Mol Brain* 2014; 7: 47–06.
15. Wang H, Xu H, Wu LJ, Kim SS, Chen T, Koga K, Descalzi G, Gong B, Vadakkan KI, Zhang X, Kaang BK and Zhuo M. Identification of an adenylyl cyclase inhibitor for treating neuropathic and inflammatory pain. *Sci Trans Med* 2011; 3: 65ra63.
16. Zhuo M. Targeting neuronal adenylyl cyclase for the treatment of chronic pain. *Drug Discov Today* 2012; 17: 573–582.
17. Chen T, Lu JS, Song Q, Liu MG, Koga K, Descalzi G, Li YQ and Zhuo M. Pharmacological rescue of cortical synaptic and network potentiation in a mouse model for fragile X syndrome. *Neuropsychopharmacol* 2014; 39: 1955–1967.
18. Li X, Matsuura T, Liu RH, Xue M and Zhuo M. Calcitonin gene-related peptide potentiated the excitatory transmission and network propagation in the anterior cingulate cortex of adult mice. *Mol Pain* 2019; 15: 1744806919832718.
19. Koga K, Liu MG, Qiu S, Song Q, O'Den G, Chen T and Zhuo M. Impaired presynaptic long-term potentiation in the anterior cingulate cortex of Fmr1 knock-out mice. *J Neurosci* 2015; 35: 2033–2043.
20. Song Q, Liu MG and Zhuo M. Minocycline does not affect long-term potentiation in the anterior cingulate cortex of normal adult mice. *Mol Pain* 2015; 11: 25.
21. Shin RM, Tully K, Li Y, Cho JH, Higuchi M, Suhara T and Bolshakov VY. Hierarchical order of coexisting pre- and postsynaptic forms of long-term potentiation at synapses in amygdala. *Proc Natl Acad Sci U S A* 2010; 107: 19073–19078.
22. Nicoll RA and Schmitz D. Synaptic plasticity at hippocampal mossy fibre synapses. *Nat Rev Neurosci* 2005; 6: 863–876.
23. Koga K, Yao I, Setou M and Zhuo M. SCRAPER selectively contributes to spontaneous release and presynaptic long-term potentiation in the anterior cingulate cortex. *J Neurosci* 2017; 37: 3887–3895.
24. Liauw J, Wu LJ and Zhuo M. Calcium-stimulated adenylyl cyclases required for long-term potentiation in the anterior cingulate cortex. *J Neurophysiol* 2005; 94: 878–882.
25. Geuze E, Westenberg HG, Jochims A, de Kloet CS, Bohus M, Vermetten E and Schmahl C. Altered pain processing in veterans with posttraumatic stress disorder. *Arch Gen Psychiatry* 2007; 64: 76–85.
26. Hubbard CS, Hong J, Jiang Z, Ebrat B, Suyenobu B, Smith S, Heendeniya N, Naliboff BD, Tillisch K, Mayer EA and Labus JS. Increased attentional network functioning related to symptom severity measures in females with irritable bowel syndrome. *Neurogastroenterol Motil* 2015; 27: 1282–1294.
27. Wiech K and Tracey I. The influence of negative emotions on pain: behavioral effects and neural mechanisms. *NeuroImage* 2009; 47: 987–994.
28. Craig AD, Chen K, Bandy D and Reiman EM. Thermosensory activation of insular cortex. *Nat Neurosci* 2000; 3: 184–190.
29. Jasmin L, Rabkin SD, Granato A, Boudah A and Ohara PT. Analgesia and hyperalgesia from GABA-mediated modulation of the cerebral cortex. *Nature* 2003; 424: 316–320.
30. Craig AD. Topographically organized projection to posterior insular cortex from the posterior portion of the ventral medial nucleus in the long-tailed macaque monkey. *J Comp Neurol* 2014; 522: 36–63.
31. Damasio AR, Grabowski TJ, Bechara A, Damasio H, Ponto LL, Parvizi J and Hichwa RD. Subcortical and cortical brain activity during the feeling of self-generated emotions. *Nat Neurosci* 2000; 3: 1049–1056.
32. Yoshihara K, Tanabe HC, Kawamichi H, Koike T, Yamazaki M, Sudo N and Sadato N. Neural correlates of fear-induced sympathetic response associated with the peripheral temperature change rate. *NeuroImage* 2016; 134: 522–531.